Clays and Clay Minerals, Vol. 38, No. 6, 561–572, 1990.

MINERALOGY, CHEMISTRY, AND DIAGENESIS OF TUFFS IN THE SUCKER CREEK FORMATION (MIOCENE), EASTERN OREGON

STEPHEN P. ALTANER AND RALPH E. GRIM†
Department of Geology, University of Illinois, Urbana, Illinois 61801

Abstract—The lacustrine Sucker Creek Formation (Miocene) of eastern Oregon includes unaltered vitric tuffs as well as tuffs altered to the following diagenetic facies: (1) bentonite, (2) interbedded bentonite and opal-CT, (3) K-clinoptilolite, and (4) Ca-clinoptilolite. Bentonite beds contain Fe-rich smectite (8–10 wt. % Fe_2O_3), quartz, plagioclase, and Ca-clinoptilolite. Opal-CT-rich layers contain inorganic silica (opal-CT), Fe-rich smectite, and minor diatoms. K-clinoptilolite beds typically contain clinoptilolite that can be extremely K-rich (≤7.6 wt. % K_2O), opal-CT, smectite, plagioclase, and K-feldspar. This diagenetic facies also includes smectitic tuff and unaltered tuff. Ca-clinoptilolite beds contain Ca-clinoptilolite, quartz, K-feldspar, smectite, and illite.

Based on its chemistry and mineralogy, the bentonite appears to have been derived from dacitic volcanic ash. Chemical considerations and the close spatial relationship between beds of bentonite and opal-CT suggest that the diagenetic alteration of glass to smectite provided silica to the adjacent opal-CT beds. Based on the presence of late-stage Ca-clinoptilolite, alteration appears to have proceeded in a relatively closed chemical system.

Based on the composition of preserved vitric tuff, the zeolitic tuffs appear to be derived from rhyolitic ash, which diagenetically altered in an open hydrologic system and produced vertical zonations in mineralogy. In this model, bentonite horizons at the top of the K-clinoptilolite diagenetic facies formed by reaction of volcanic glass with dilute fluids that had a relatively low $(Na^+ + K^+ + Ca^{2+})/H^+$ activity ratio and $a_{H_4SiO_4}$, whereas the underlying K-clinoptilolite beds formed from reactions between glass and dilute fluids having a higher $(Na^+ + K^+ + Ca^{2+})/H^+$ activity ratio and $a_{H_4SiO_4}$. Unaltered vitric ash between these beds may represent zones of higher permeability that inhibited secondary mineral alteration. Ca-clinoptilolite-rich beds appear to have undergone alteration similar to K-clinoptilolite-rich beds as well as to have been subjected to later, low-temperature (perhaps 75°–150°C) hydrothermal alteration which enhanced cation exchange in the zeolite and formed quartz from opal-CT.

Key Words—Clinoptilolite, Diagenesis, Opal-CT, Smectite, Tuff, Zeolites.

INTRODUCTION

The Sucker Creek Formation (Late Miocene) includes numerous tuffs that contain a variety of alteration assemblages, including smectite (bentonite), opal-CT, and clinoptilolite. These units are well exposed in the Succor Creek canyon area[1] of eastern Oregon. The mineralogical and chemical differences among the tuffs reflect differences in both the composition of the precursor volcanic ash and diagenetic fluids.

The clinoptilolite-rich beds and bentonite beds are interesting not only from a geological perspective, but also from an economic perspective, because both are currently mined by Teague Mineral Products, Adrian, Oregon. The clinoptilolite-rich tuff has a high cation-exchange capacity and excellent cation-selectivity characteristics. It is reported to be used for environmental and agricultural purposes including: to solidify and stabilize hazardous waste, for odor control, to improve nutrient uptake in soils, as an anticaking agent, and as an animal feed supplement (Leppert, 1990). The bentonite is used as a soil sealant to retard chemical migration in hazardous waste sites and sewage lagoons and as a dairy feed supplement and a drilling mud.

The purpose of this paper is to characterize the mineralogy, chemistry, and texture of the altered tuffaceous rocks in the Sucker Creek Formation and to discuss the mode of origin for each diagenetic facies.

GEOLOGIC SETTING

The Succor Creek area of eastern Oregon is located in the Owyhee River region, which is the northeastern extremity of the Basin and Range physiographic province. This area consists of rugged uplands having an average elevation of about 1.4 km and an average annual rainfall of about 25 cm. The region is dominated structurally by tilted block faults having a general northerly trend. The rocks of the Owyhee River region are Miocene through Pleistocene in age and consist of flat-lying or gently dipping volcaniclastic and extrusive volcanic rocks, which range in composition from basalt to rhyolite (Kittleman *et al.*, 1965). The following geologic description of the Owyhee River region and the

† Deceased, August 19, 1989.

[1] Succor Creek refers to the stream that flows through the east-central Oregon area, and Sucker Creek Formation refers to the geologic formation described in this article.

Sucker Creek Formation is based largely on Kittleman *et al.* (1965) and Kittleman (1973).

In the Middle Miocene, extensive basalt flows and rhyolite extrusions formed the structural foundation for later accumulation of volcanic materials. Due to crustal extension later in the Miocene, the basal volcanic platform was deformed by north-trending step faults, which resulted in the formation of elongate basins. Deposition began in the Late Miocene and continued with local interruption into the Pliocene. Deposits include volcanic ash layers, ash-flow tuff, thin basalt flows, sandstone, arkose, and conglomerate. Most of these basins were filled by Middle Pliocene time and then capped by basalt flows in the Late Pliocene and Pleistocene.

The Sucker Creek Formation (Late Miocene) consists mainly of lacustrine volcaniclastic rocks and tuff, which were deposited in a moist temperate lowland climate (<300 m elevation, Kittleman, 1973). These strata are exposed locally along Succor Creek, located near the border of Oregon and Idaho (Figure 1) and are among the oldest strata deposited in the Owyhee River region. The total thickness of the Sucker Creek Formation is difficult to estimate because of extensive faulting, but is about 500 m. An apparent unconformity separates a shallow-dipping (10°–20°) lower member from a flat-lying upper member (D. Leppert, Adrian, Oregon, personal communication, 1987). The lower member contains the zeolite and interbedded bentonite-opal-CT units, whereas the upper member contains the bentonite unit.

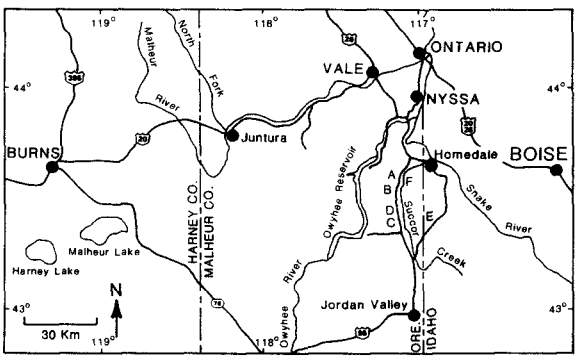

Figure 1. Locality map of east-central Oregon. Letter represents sampled locality (sections A–F) of Sucker Creek Formation.

METHODS

Fifty-five samples from six sections (labeled A through F in Figure 1) of the Sucker Creek Formation in eastern Oregon and western Idaho were studied. The sections were particularly well exposed because they are presently being mined or have recently been mined. Section A, from the GB pit, represents the bentonite diagenetic facies. Sections B and C, from the B and BLM pits, respectively, represent the interbedded bentonite-opal-CT diagenetic facies. Sections D and E, from the Zeogroup and Chrisman Hill pits, represent the K-clinoptilolite diagenetic facies. Section F, from the Succor Creek pit, represents the Ca-clinoptilolite diagenetic facies. Sample labels in the tables include sample number and the last two digits of the year in which the sample was collected (86 or 87).

X-ray powder diffraction (XRD) data were determined using a Siemens D-500 powder diffractometer equipped with a copper tube and a graphite monochromator. Scanning speeds for all samples were 2°2θ/min. Bulk samples were ground to pass a 325 mesh sieve, side-loaded into an aluminum holder, and X-rayed to determine whole sample mineralogy. Unit-cell parameters of clinoptilolite (samples 7-87 and 26-86, Table 3) were calculated using digitized XRD data and a Rietveld refinement program (Wiles and Young, 1981). Unit-cell parameters of clinoptilolite sample 2-87 (containing quartz as an internal calibrant) were calculated using strip-chart XRD data and the cell-refinement program of Appleman and Evans (1973). The thermal stability of selected zeolite samples was determined by XRD analysis of powders heated at 450°C for 16 hr. The <1-μm size fraction was obtained by centrifugation, concentrated onto a Millipore filter by vacuum suction, and transferred onto a glass slide. To determine the clay mineralogy, the glass slide was examined after air-drying and after solvation with ethylene glycol. Mineral abundances in bulk samples were calculated using intensity factors listed in Hoffman (1976) and Bayliss (1986). Abundances of clay minerals (<1-μm size fraction) were calculated using intensity factors from Reynolds (1989). Estimated error for these analyses is 30% of the amount present and at least 50% of the amount present for minerals which comprise <10% of the sample (Bayliss, 1986). The coarse-size fraction of selected bentonites was obtained by dispersing the sample in water and decanting the suspended material. Plagioclase compositions were determined using immersion oil and an optical microscope. The abundance of volcanic ash was estimated by examination with an optical microscope.

Thin sections of samples were examined with an optical microscope, and rock chips were examined with a scanning electron microscope (JEOL JSM-840A) equipped with an energy-dispersive X-ray analyzer (Kevex 7500). Polished thin sections of several samples were analyzed with a microprobe (JEOL 50AX) equipped with an energy-dispersive X-ray analyzer (Tracor Northern TN-2000). Spectra were collected for 120 s (live time) using an electron beam of 300 pA, 20 keV, and ~1 μm in diameter. The following elements were compared with standards: Si, Al, Ti, Fe, Mg, Ca,

Table 1. X-ray powder diffraction mineralogy of representative samples from the Sucker Creek Formation.

Sample	Cp[1]	Clay[2]	Opal	Qtz	Kspar	Pf	Glass
Section A. Bentonite							
Upper green bent. (2-86)[3]	—	83[4]	4	13	—	—	—
Middle green coarse bent. (2-87)	57	35	—	2	—	6	—
Lower brown bent. (1-87)	—	88	—	9	—	3	—
Section B. Interbedded bentonite-opal-CT							
Siliceous bed (9-87)	—	39	54	1	—	5	—
Brown bent. (10-87)	—	64	24	2	—	9	—
Siliceous bed (11-87)	—	57	37	—	—	6	—
Brown bent. (12-87)	39	35	trace	13	—	11	—
Siliceous bed (13-87)	—	40	60	—	—	—	—
Green bent. (14-87)	—	91	—	2	—	7	—
Section C. Interbedded bentonite-opal-CT							
Siliceous bed (29-87)	51	41	4	1	—	3	—
Siliceous bed (14-86)	—	41	46	3	—	10	—
Bentonite (15-86)	—	83	—	10	7	—	—
Bentonite (28-87)	42	56	trace	—	—	2	—
Section D. K-clinoptilolite							
Bentonite (12-86)	57	38	trace	2	—	3	—
Bentonite (25-87)	—	92	8	—	—	—	—
Gray ash (11-86)	<5	<5	trace	trace	—	trace	90
Zeolite (26-87)	84	—	6	3	—	7	—
Section E. K-clinoptilolite							
Bentonite (32-87)	—	80	—	6	9	—	5
Gray ash (31-87)	—	12	—	trace	7	—	80
Zeolite (26-86)	72	12	trace	1	3	12	—
Section F. Ca-clinoptilolite							
Bentonitic bed (6-87)	45	32	—	17	5	—	—
Zeolite (7-87)	79	14	—	7	—	—	—

[1] Cp = clinoptilolite, Clay = total clay minerals, Opal = opal-CT, Qtz = quartz, Kspar = K-feldspar, Pf = plagioclase feldspar, and Glass = volcanic glass.

[2] The clay minerals in nearly all samples are pure smectite. Samples 6-87 and 7-87 of section F contain illite as well as smectite.

[3] Sample labels include a collection number and the last two digits of the year of collection.

[4] Numbers represent mineral abundance in terms of weight percent.

Na, K, and Ba. Calculated oxide abundances were corrected for matrix effects using a "Magic"-type correction program. Fe was assumed to be in the ferric oxidation state. Selected samples were ground to pass a 200 mesh sieve and analyzed by X-ray fluorescence (XRF) at a commercial laboratory (X-ray Assay Laboratory, Don Mills, Ontario).

RESULTS

Bentonite diagenetic facies

The bentonite diagenetic facies (section A) contains four distinct nearly horizontal beds of green and brown bentonite. The section from top to bottom consists of green bentonite (~15 m thick) containing coarse sand-size to cobble-size white concretions and green rock fragments, light-green coarse-grained tuff (~2 m thick) containing coarse sand-size concretions, green bentonite (1–2 m thick) containing few coarse particles, and dark brown bentonite (7–9 m thick) lacking coarse particles. The basal brown bentonite (sample 1-87 in Tables 1 and 2) is currently mined by Teague Mineral Products. Drillholes that penetrated below the basal brown bentonite encountered hard (silica-rich?) layers of variable thickness.

The mineralogy of the bentonite beds (Table 1) is typically dominated by smectite and also includes opal-CT, clinoptilolite, and minerals of both detrital and pyrogenic origin (quartz and plagioclase). Figure 3A shows a representative XRD pattern of the basal brown bentonite, which reveals a turbostratic stacking arrangement, typical for smectite. The smectite 060 spacing is 1.500–1.504 Å. XRD analysis of oriented, ethylene glycol-treated, <1-μm size separates showed the presence of pure smectite containing no interstratified illite layers.

The zeolite was identified as Ca-clinoptilolite because its unit-cell volume was similar to values for other clinoptilolite samples, its peak intensities decreased significantly after a 450°C heat treatment, and no heulandite-B phase formed on heating (Table 3). For example, the 020 peak intensity decreased by 60–

https://doi.org/10.1346/CCMN.1990.0380601 Published online by Cambridge University Press

Table 2. Chemical composition of representative tuffs from the Sucker Creek Formation based on X-ray fluorescence analyses.[1]

Sample	SiO_2	Al_2O_3	TiO_2	Fe_2O_3	MnO	MgO	CaO	K_2O	Na_2O	LOI	Sum	Rb	Sr	Ba
Section A. Bentonite														
Upper bent. (2-86 A)	51.8	13.7	1.00	8.03	0.02	1.45	1.18	0.68	0.95	20.80	99.7	52	64	147
Lower bent. (1-87 A)	53.5	17.0	1.25	6.75	0.01	1.46	1.32	0.70	1.11	16.20	99.4	40	96	149
Section B. Interbedded bentonite-opal-CT														
Silic. bed (9-87 B)	82.9	5.4	0.40	1.93	0.01	0.44	0.50	0.30	0.66	6.23	98.9	32	44	75
Brown bent. (10-87 B)	58.3	15.7	1.16	6.37	0.01	1.16	1.13	0.62	1.17	13.80	99.6	39	80	148
Silic. bed (11-87 B)	66.5	11.9	0.93	4.68	0.01	1.04	1.08	0.60	1.17	10.50	98.6	37	101	128
Brown bent. (12-87 B)	61.2	14.7	1.01	5.98	0.01	1.05	1.05	0.86	1.26	13.2	100.5	48	77	154
Silic. bed (13-87 B)	78.5	7.4	0.53	2.98	0.01	0.62	0.50	0.35	0.87	7.54	99.3	26	29	92
Green bent. (14-87 B)	55.2	18.5	0.37	6.54	0.02	0.89	2.12	1.99	2.61	11.10	99.5	41	273	169
Section C. Interbedded bentonite-opal-CT														
Silic. bed (29-87)	68.0	11.5	0.31	4.02	0.09	0.83	1.27	1.04	0.85	12.0	100.1	57	201	282
Bent. (28-87)	61.5	12.4	0.31	7.48	0.21	1.16	1.48	0.50	0.58	14.4	100.2	31	94	387
Section D. K-clinoptilolite														
Bent. (12-86)	64.4	12.6	0.40	3.58	0.01	0.76	1.41	2.65	1.24	11.90	99.2	117	233	217
Bent. (25-87)	61.4	12.2	0.42	5.89	0.03	1.19	1.41	1.41	1.03	15.1	100.3	86	60	296
Gray ash (11-86)	68.4	10.6	0.28	2.53	0.05	0.33	0.99	3.66	1.41	10.20	98.7	220	41	788
Zeolite (26-87)	71.5	9.6	0.31	2.20	0.01	0.50	1.02	2.58	1.18	9.77	99.0	117	206	2480
Section E. K-clinoptilolite														
Zeolite (26-86)	66.5	11.4	0.32	2.15	0.02	0.20	0.98	4.78	1.41	11.60	99.7	216	191	1680
Section F. Ca-clinoptilolite														
Bentonitic bed (6-87)	60.4	13.6	0.35	3.50	0.02	1.03	2.12	2.99	0.96	14.60	99.9	112	469	847
Zeolite (7-87)	65.5	11.9	0.25	2.32	0.01	0.85	3.01	1.70	1.12	12.60	99.6	119	584	1480

[1] Values for SiO_2 through sum are in terms of weight percent, and values for Rb through Ba are in ppm. Fe is assumed to be Fe_2O_3. Loss on ignition (LOI) was determined at 960°C for 1 hr.

Table 3. Electron microprobe analyses, unit-cell, and thermal stability data for montmorillonite (Mont.) and clinoptilolite (Cp) from the Sucker Creek Formation.

	2-86-A[1] (Mont.)	12-86-D (Mont.)	12-86-D (K-Cp)	26-86-E (K-Cp)	7-87-F (Ca-Cp)	2-87-A (Ca-Cp)
SiO_2	54.39	53.34	62.65	65.58	62.72	
Al_2O_3	16.59	20.49	11.90	11.62	12.03	
TiO_2	0.50	0.70	n.d.[2]	n.d.	n.d.	
Fe_2O_3[3]	9.73	6.89	n.d.	n.d.	0.22	
MgO	1.82	1.36	0.49	n.d.	0.74	
CaO	1.11	0.63	1.95	0.98	3.76	
K_2O	0.53	2.72	3.55	7.62	0.51	
Na_2O	1.15	0.86	1.64	1.16	1.36	
Sum	85.82	86.91	82.18	86.96	81.34	
	Cations based on 11 oxygens		Cations based on 72 oxygens			
Si	3.86	3.74	29.48	29.71	29.38	
Al	1.38	1.70	6.60	6.19	6.63	
Ti	0.03	0.04	—	—	—	
Fe	0.52	0.36	—	—	0.08	
Mg	0.19	0.14	0.35	—	0.52	
Ca	0.08	0.05	1.00	0.48	1.89	
K	0.05	0.24	2.10	4.41	0.31	
Na	0.16	0.12	1.50	1.02	1.23	
Unit-cell dimension						
a (Å)				17.636	17.642	17.68
b (Å)				17.843	17.907	17.86
c (Å)				7.394	7.401	7.43
β (°)				116.29	116.43	116.5
Volume (Å^3)				2086.5	2093.7	2100.3
Thermal stability[4]				C	I	I

[1] Letter in sample label indicates section (A–F).
[2] n.d. represents not detected.
[3] Fe assumed as Fe_2O_3.
[4] Thermal stability refers to change in X-ray powder diffraction pattern after heating at 450°C for 16 hr. C = No change in d-values and minor intensity loss. I = Change in d-values and major loss of intensity.

70% after the 450°C heating. Previous investigators have found that the exchangeable cation affects the thermal stability of clinoptilolite, i.e., Ca-exchanged clinoptilolite is relatively thermally unstable, whereas K-exchanged clinoptilolite is thermally stable (Shepard and Starkey, 1966; Gottardi and Galli, 1985). Because the clinoptilolite is intimately intermixed with the smectite, however, we were unable to obtain meaningful microprobe analyses to determine the Si/Al ratio for the zeolite.

Scanning electron microscopy (SEM) revealed that the smectite in these beds has a delicate cornflake morphology (Figure 4A), typical of smectite minerals. Optical microscopy and SEM analyses showed no relict shard structures; however, rounded masses of smectite were noted and may have formed from pellets of volcanic ash. Both detrital and pyrogenic forms of quartz and plagioclase occur in the bentonite. Pyrogenic plagioclase has a composition of An_{30-35}. Ca-clinoptilolite occurs as small (~3–5 μm), tabular, euhedral grains in the white concretions and in small cavities within the smectite matrix.

Table 2 shows XRF analyses of the upper and lower bentonites, which contain high Fe_2O_3 contents (7–8 wt. %) and relatively low MgO and Al_2O_3 contents (~1.5 wt. % and 13.7–17 wt. %, respectively), compared with typical bentonites. For example, the Otay, Upton, and Polkville bentonites have the following range in composition: 0.9–4 wt. % Fe_2O_3, 2.5–6.5 wt. % MgO and 16–20 wt. % Al_2O_3 (Ross and Hendricks, 1945). Based on microprobe analyses of the smectite in the bentonite (Table 3), Fe occupies ~25% of the octahedral sites, the total layer charge is low (−0.36), and Na is the predominant interlayer cation. This smectite was therefore classified as an Fe-rich montmorillonite.

Interbedded bentonite-opal-CT diagenetic facies

The interbedded bentonite-opal-CT diagenetic facies is represented in sections B and C as soft layers of green and brown bentonite (similar to the bentonite in section A), which are interbedded with hard, white layers rich in opal-CT. Section B contains a basal bentonite (6 m thick), mined by Teague Mineral Products, which is overlain by at least five pairs of bentonite and opal-CT-rich beds, which range in individual thickness from 10 to 20 cm. Samples 9-87 through 14-87 in Tables 1 and 2 are from these thin bentonite-opal-CT pairs. Section B is shown diagrammatically in Figure 2A. Section C contains a 2-m-thick layer of green bentonite overlain by a 3–4-m-thick white, siliceous bed.

https://doi.org/10.1346/CCMN.1990.0380601 Published online by Cambridge University Press

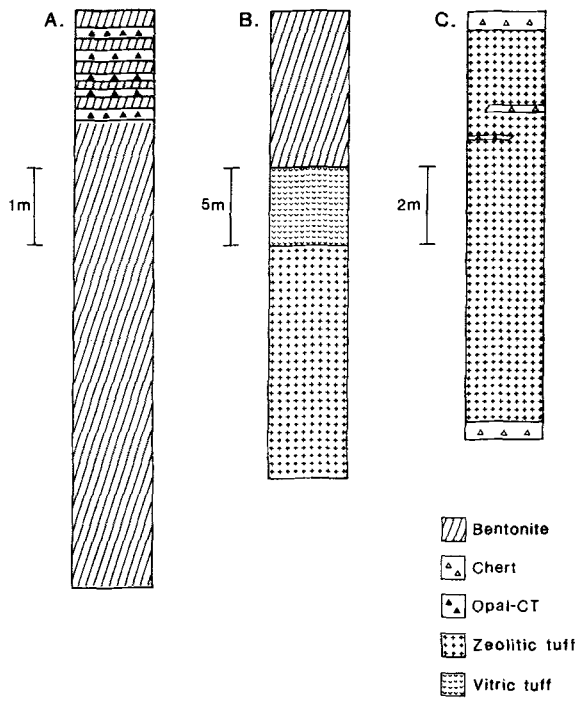

Figure 2. Columnar sections of representative diagenetic facies of the Sucker Creek Formation. A. Interbedded bentonite-opal-CT (section B), B. K-clinoptilolite (section E), C. Ca-clinoptilolite (section F).

The mineralogy of the bentonite beds in the interbedded bentonite-opal-CT diagenetic facies is similar to the pure bentonite facies described above, containing mostly smectite and minor amounts of opal-CT, detrital and pyrogenic minerals (plagioclase and quartz), and locally Ca-clinoptilolite (Table 1). One bentonite bed from section C (sample 15-86, Table 1) contains ~7% K-feldspar of probable low-temperature origin based on its XRD pattern and its fine-grained nature in thin section (Sheppard and Gude, 1973). The opal-CT beds contain more opal-CT and less smectite than the bentonite beds. The white siliceous layer at section C contains variable amounts of Ca-clinoptilolite and opal-CT (Table 1). Figure 3B shows a representative XRD pattern of a sample rich in opal-CT (broad peaks at 4.29, 4.07, and 2.49 Å). The XRD characteristics of the smectite and clinoptilolite in the interbedded bentonite-opal-CT beds are similar to those described above for the pure bentonite beds.

SEM analysis revealed that the layers rich in opal-CT contain both diagenetic silica and organically precipitated silica. Organic silica is represented by abundant diatoms (Figure 4B), and diagenetic silica is represented by abundant opal-CT spheres, which contain short, stubby crystals (Figure 4C) and acicular crystals. Diatoms also have smectite growths on top of them (Figure 4D). Fibers that resemble mordenite (Figure 4E) were detected in one opal-CT bed from section

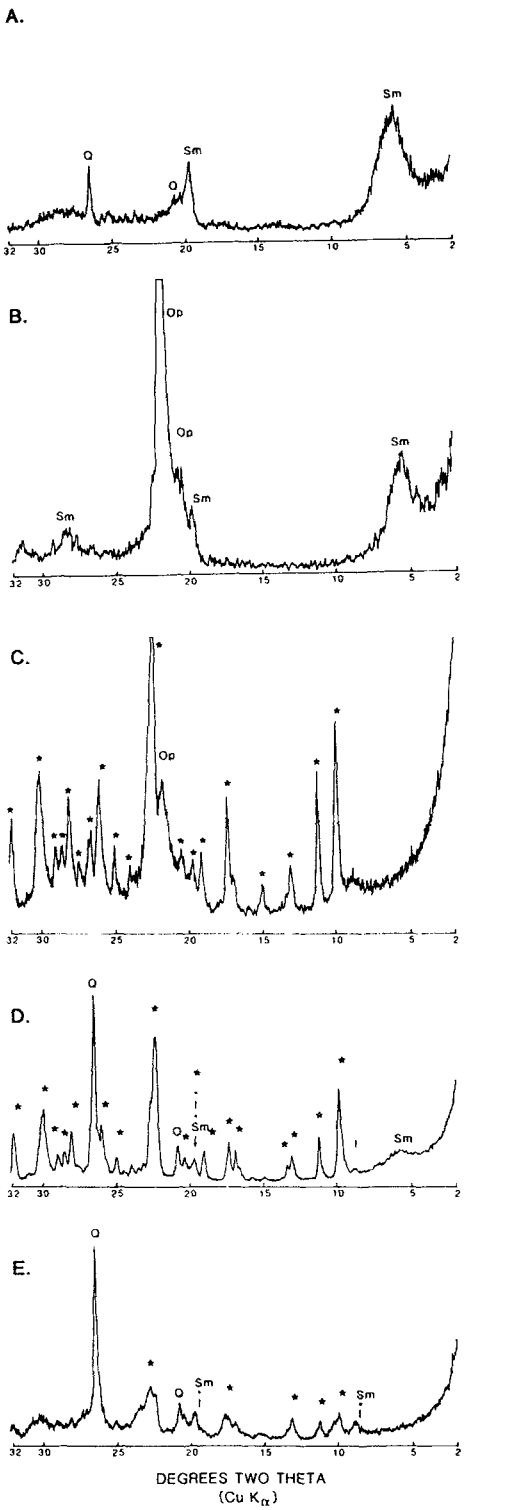

Figure 3. X-ray powder diffraction patterns of representative samples from four diagenetic facies of the Sucker Creek Formation. A. Bentonite, B. Opal-CT, C. K-clinoptilolite, D. Ca-clinoptilolite, E. Ca-clinoptilolite heated at 450°C for 16 hr. Sm = smectite, Q = quartz, Op = opal-CT, * = clinoptilolite, I = illite.

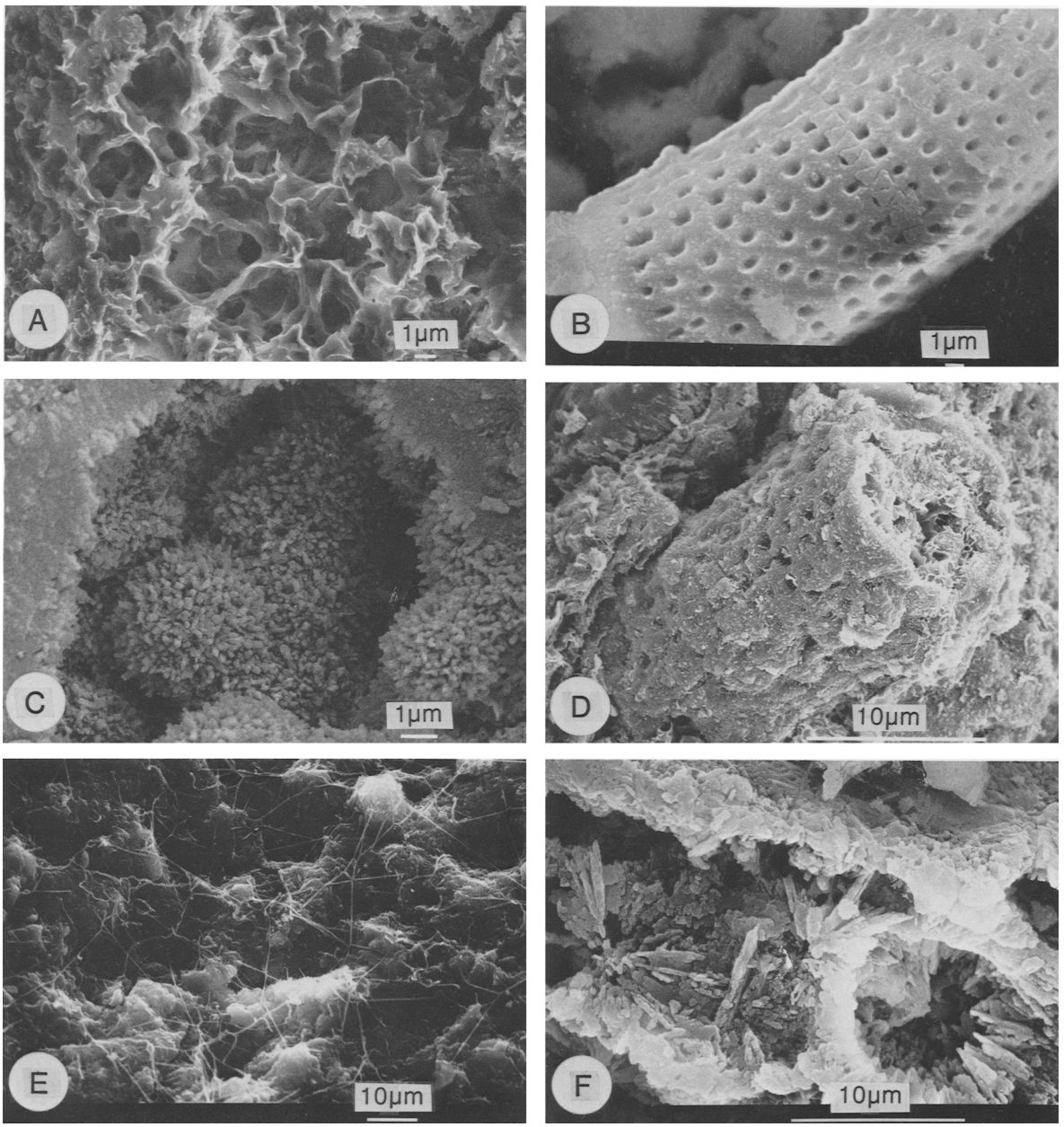

Figure 4. Scanning electron microscope photographs of clay and siliceous minerals from the Sucker Creek Formation. A. Smectite from bentonite bed, B. Diatom from opal-CT-rich bed, C. Inorganically precipitated silica (opal-CT) from opal-CT-rich bed, D. Diatom from opal-CT-rich bed with smectite growing on it, E. Fibrous mordenite(?) from opal-CT-rich bed, F. Quartz from Ca-clinoptilolite unit.

B. Smectite and clinoptilolite in the interbedded bentonite-opal-CT beds have morphologies similar to those in the pure bentonite beds.

The white opal-CT-rich beds contain much more SiO_2 (as much as 83 wt. % SiO_2) and lesser amounts of all other oxides and elements, compared with the interbedded bentonites (Table 2). The composition of interbedded bentonites (high Fe and relatively low Mg and Al) is similar to those of the pure bentonite diagenetic facies.

K-clinoptilolite diagenetic facies

The K-clinoptilolite facies is represented by sections D and E, which show the following zonation: a 10–15-m-thick unit of clinoptilolite-rich tuff near the base of the section, an overlying 3–5-m-thick unit of substan-

https://doi.org/10.1346/CCMN.1990.0380601 Published online by Cambridge University Press

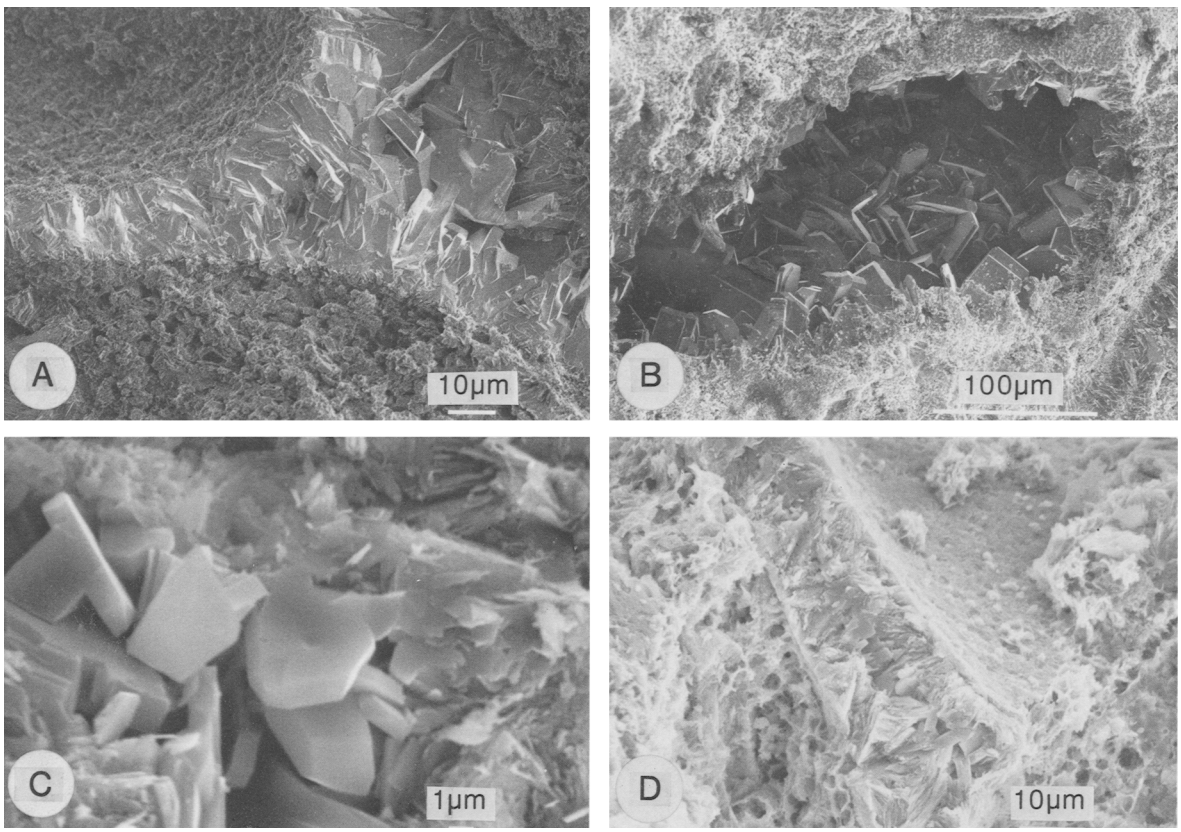

Figure 5. Scanning electron microscope photographs of zeolites from clinoptilolite tuff of the Sucker Creek Formation. A. K-clinoptilolite replacing shard, B. K-clinoptilolite filling vug, C. Ca-clinoptilolite filling vug, D. Ca-clinoptilolite replacing shard.

tially unaltered vitric ash, and a 10–12-m-thick unit of bentonite at the top of the section. Section E is shown diagrammatically in Figure 2B. In section D, a 10-m-thick bed of silty limestone underlies the clinoptilolite-rich tuff. The clinoptilolite-rich beds also contain localized clay-rich zones and have a sharp transition to the overlying vitric ash. The boundary between the ash and bentonite layers is more gradational, consisting of a broad (1–2 m) interval of mixed ash and clay.

The zeolite beds are dominated by clinoptilolite, with minor amounts of smectite, opal-CT, and detrital and pyrogenic minerals (plagioclase, sanidine, and quartz; Table 1). Figure 3C shows a representative XRD pattern of the clinoptilolite bed from section E. This sample showed only slight change after a 450°C heat treatment (the 020 peak was reduced by about 10%), which is typical of K-rich clinoptilolite (Shepard and Starkey, 1966). Unit-cell parameters are also typical for clinoptilolite (Table 3). The slightly altered vitric ash layers contain abundant volcanic glass, as well as some detrital and pyrogenic minerals (quartz and sanidine) and diagenetic minerals (smectite and clinoptilolite). The bentonite beds contain abundant smectite, variable amounts of clinoptilolite and volcanic glass, and minor amounts of opal-CT, quartz, and plagioclase. The XRD characteristics of the smectite are similar to those described for the bentonite beds.

SEM analyses revealed that clinoptilolite, with its characteristic tabular shape, has replaced bubble-wall shards (Figure 5A) and long tubular shards, and has also filled vugs (Figure 5B) and veins. The pseudomorphs of shards replaced by clinoptilolite were also clearly visible by optical microscopy. The clinoptilolite-rich tuff has a more massive texture where the clinoptilolite completely fills pore spaces. Smectite and opal-CT, having morphologies similar to those in the bentonite and opal-CT units, typically form outlines of shards and appear to have preceded the formation of the zeolite.

XRF analyses of the zeolitic tuffs show high Si, Al, K, and Ba contents and relatively low Fe, Mg, Ca, and Na contents (Table 2). Clinoptilolite from section E contains significantly more K_2O than does the clinoptilolite from section D (4.78 vs. 2.58 wt. %). The chemical composition of the vitric ash from section D (sample 11-86) is very similar to compositions of the clinoptilolite-rich beds. The relatively high weight loss on ignition (10.2 wt. %) for the vitric ash supports the

https://doi.org/10.1346/CCMN.1990.0380601 Published online by Cambridge University Press

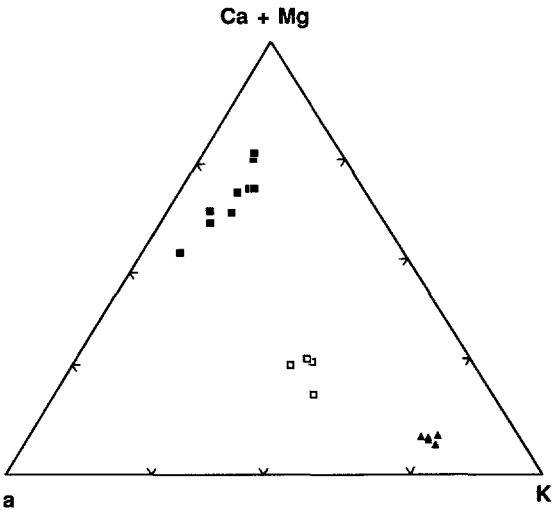

Figure 6. Zeolite compositions from microprobe analyses plotted on a ternary Na-K-(Ca + Mg) composition diagram. Solid squares represent clinoptilolite from Ca-clinoptilolite tuff, open squares and triangles represent clinoptilolite from K-clinoptilolite tuff (section D and E, respectively).

XRD data, which show that some clay and zeolite alteration has occurred in the vitric ash. The most clay-rich bed of the bentonitic layers (sample 25-87 of section D) contains more Fe, Mg, and Al and less Si, K, Sr, and Ba than the underlying clinoptilolite bed.

Microprobe analyses showed that clinoptilolite from section D has a typical clinoptilolite composition, whereas that from section E has an extremely high K_2O content (7.62 wt. %, Table 3), supporting XRF analyses of bulk samples. Structural formulae (Table 3) indicate that the clinoptilolite from sections D and E have similar Si/Al ratios (4.47 and 4.80, respectively) and that clinoptilolite from section E has a much higher K/Na ratio than clinoptilolite from section D (4.32 and 1.40, respectively). Smectite from section D has less Fe, Mg, Ca, and Na, and more Al and K compared with smectite from the bentonite diagenetic facies.

Ca-clinoptilolite diagenetic facies

The Ca-clinoptilolite-rich tuff, represented by section F (shown diagrammatically in Figure 2C, is ~10 m thick and consists mostly of clinoptilolite-rich strata. Two, 0.5-m-thick layers of gray-blue chert are present, one at the top and one at the bottom of the section. In addition, discontinuous veins of tan chert occur throughout this section.

Both the zeolite and bentonitic horizons contain clinoptilolite as the major mineral with lesser amounts of smectite, illite, quartz, and detrital and pyrogenic K-feldspar (Table 1). Figure 3D shows a representative XRD pattern of the Ca-clinoptilolite bed from section F. This sample was significantly affected by the 450°C heat treatment (the 020 peak was reduced by about 76%, Figure 3E); however, no heulandite-B phase formed. These characteristics are compatible with the thermal stability of Ca-clinoptilolite (Shepard and Starkey, 1966). Unit-cell parameters for Ca-clinoptilolite sample 7-87 are similar to the other clinoptilolite minerals examined in the present study (Table 3). The Ca-clinoptilolite-rich tuffs are unusual in that both illite and smectite coexist with the clinoptilolite. Clay-size fractions contain between 5 and 23% illite; the remainder is smectite.

The texture of the Ca-clinoptilolite is similar to that of the K-clinoptilolite, with tabular crystals replacing bubble-wall shards (Figure 5D) and filling pore spaces (Figure 5C). Shard pseudomorphs were also readily apparent by optical microscopy. Clays and quartz typically outline shards and appear to have formed prior to clinoptilolite. Quartz occurs as ~1-μm-thick acicular particles (Figure 4F), which are typically wider than the acicular, <0.5-μm-thick particles of opal-CT in other altered tuffs.

XRF analyses of zeolite samples from the Ca-clinoptilolite diagenetic facies are similar to zeolite samples from the K-clinoptilolite diagenetic facies, except for somewhat lower Si and K contents, and higher Ca, Al, Mg, and Sr contents (Table 2). Microprobe analyses revealed that Ca-clinoptilolite from section F has more Ca and less Na and K than the K-clinoptilolite (Table 3). The Si/Al ratios for the K- and Ca-clinoptilolite are similar. Chemical differences among the one Ca-clinoptilolite and two K-clinoptilolite samples are clearly shown in the ternary diagram, Na-K-(Ca + Mg) (Figure 6).

DISCUSSION

Origin of the bentonite diagenetic facies

The abundance of pure smectite and presence of sand-size igneous materials (pyrogenic quartz and plagioclase) clearly indicates that bentonite in both the pure bentonite and the interbedded bentonite-opal-CT facies was derived from a volcanic precursor. Opal-CT-rich beds are interpreted to represent silica-rich layers, which were produced during the diagenetic alteration of volcanic ash to smectite, based on the close spatial relationship between the bentonite and opal-CT beds, and the authigenic morphology of the opal-CT. The composition of the precursor volcanic ash is difficult to determine because of the absence of preserved volcanic glass in these beds; however, the composition may have been dacitic, based on the presence of pyrogenic plagioclase of andesine composition (An_{30-35}) and the chemical composition of the bentonite. The Fe content of bentonite (6–8% Fe_2O_3) from the Sucker Creek Formation is much higher than that of typical rhyolite, but it is similar to the Fe contents of dacite and andesite (Fisher and Schmincke, 1984). A direct comparison of the bentonite composition with possible

https://doi.org/10.1346/CCMN.1990.0380601 Published online by Cambridge University Press

volcanic precursors, however, is difficult to make, because of the probable mobility of silica, alkali and alkaline earth cations, and water during alteration (Slaughter and Earley, 1965).

Table 4 presents the gains and losses of chemical constituents as a result of alteration of different volcanic precursors to an average composition of bentonite from the Sucker Creek Formation. Assuming constant Al_2O_3, alteration of rhyolitic ash to bentonite would produce about 30 g of excess SiO_2 per 70 g of bentonite, whereas alteration of dacite would produce only 6.5 g of excess SiO_2 per 105 g of bentonite. The relatively small percentage of opal-CT-rich beds in sections A and B seems to support a dacitic rather than a rhyolitic precursor for the bentonite diagenetic facies. Although section C has more siliceous layers, XRD analysis revealed that the siliceous beds were compositionally heterogeneous, having local clinoptilolite-rich horizons and opal-CT-rich horizons (Table 1). Further sampling of this locality is needed to determine the mineralogical composition of the siliceous bed.

The presence of Ca-clinoptilolite in the bentonite and opal-CT-rich beds as a late-stage authigenic phase suggests that bentonite formed in a relatively closed chemical system. The formation of clinoptilolite required a higher $(Na^+ + K^+ + Ca^{2+})/H^+$ activity ratio and $a_{H_4SiO_4}$ than the formation of smectite and was enhanced by the closed-system alteration of volcanic glass to smectite, which increases cation and silica activities as well as pH. The presence of Ca-clinoptilolite, rather than of Na- or K-clinoptilolite, is compatible with a dacitic volcanic precursor. The formation of bentonite tuff at the water-sediment interface has not been documented in modern lakes, hence, the Sucker Creek tuffs probably altered to bentonite during diagenesis. For example, the youngest reported ages of bentonite tuff are about 3 Ma in both Searles Lake and the Armagosa desert (Hay *et al.*, 1986; Hay and Guldman, 1987).

In both the pure bentonite and the interbedded bentonite-opal-CT units of section A and B, smectite formation was favored by relatively dilute fluids having a relatively low $(Na^+ + K^+ + Ca^{2+})/H^+$ activity ratio (see, for example, Figures 6–8 and 6–9 in Drever, 1988). Possibly, diagenetic fluids in section C were more saline, based on the local occurrence of authigenic K-feldspar. Boles and Surdam (1979) observed coexisting smectite and K-feldspar in tuff from the Eocene Wagon Bed Formation of Wyoming, which they interpreted to be the result of diagenesis by saline, but not alkaline, pore fluids.

Origin of the clinoptilolite diagenetic facies

K-clinoptilolite (from sections D and E), Ca-clinoptilolite (from section F), and bentonite (from sections D, E, and F) formed from volcanic ash that was more silicic than the volcanic precursor of the bentonite.

Table 4. Chemical analyses of bentonite from the Sucker Creek Formation and possible volcanic precursors.[1]

	Bentonite	Rhyolite	I	Dacite	II
SiO_2	57.12	69.48	39.97[2]	66.36	59.86
Al_2O_3	15.39	10.77	10.77	16.12	16.12
TiO_2	0.85	0.28	0.59	0.58	0.89
Fe_2O_3	6.89	2.57	4.82	4.80	7.22
MnO	0.05	0.05	0.03	—	0.05
MgO	1.20	0.33	0.84	1.74	1.26
CaO	1.39	1.01	0.97	4.29	1.46
K_2O	0.89	3.72	0.62	2.22	0.93
Na_2O	1.29	1.43	0.90	3.89	1.35
LOI	14.96	10.36	10.47	—	15.67
Sum	100.0	100.0	70.0	100.0	104.8

[1] Bentonite = average of six bentonite compositions from Table 2 (sectios A, B, and C), normalized to 100%. Rhyolite = composition of gray ash (sample 11-86 of section D, Table 2) normalized to 100%. I = composition of average bentonite in first column, assuming constant Al_2O_3 of rhyolite. Dacite = composition of dacite from Fisher and Schmincke (1984). II = composition of average bentonite of first column, assuming constant Al_2O_3 of dacite.

[2] Values in columns I and II which are less than the composition of the volcanic precursor represent a net loss of oxide due to alteration, and larger values represent a net gain as a result of alteration.

Evidence for this interpretation is silicic vitric ash (close to rhyolite in composition), which is preserved in the sections that contain K-clinoptilolite, and the presence of abundant shard pseudomorphs now replaced by both K- and Ca-clinoptilolite. In addition, preserved volcanic glass in a bentonite-rich sample from section E (32-87, Table 1) has an index of refraction of 1.50, which is compatible with a rhyolitic precursor.

The probable conditions of formation for the clinoptilolite facies are: alteration in a hydrologically closed system or in a hydrologically open system. Closed hydrologic systems form in modern closed basins, such as block-faulted regions and rift valleys, in which evaporation rates exceed precipitation rates (Surdam, 1977). Fluids in the middle of the basin have greater salinities and $(Na^+ + K^+ + Ca^{2+})/H^+$ activity ratios than fluids at basin margins, due to greater amounts of evaporation and greater fluid-rock interactions. Lateral variations in mineralogy exist in closed hydrologic systems, the ideal sequence ranging from fresh glass at lake margins, to clinoptilolite (±smectite), analcime, and then K-feldspar at progressively closer intervals to the center of the basin. Modern and ancient examples of hydrologically closed systems include Teels Marsh, Nevada (Holocene, Taylor and Surdam, 1981), Lake Tecopa, California (Pleistocene, Sheppard and Gude, 1968), and the Green River Formation, Wyoming (Eocene, Hay, 1966; Surdam and Parker, 1972).

Open hydrologic systems form by the progressive increase in salinity and $(Na^+ + K^+ + Ca^{2+})/H^+$ activity ratio for meteoric water due to increasing fluid-rock interaction along a flow path (Hay and Sheppard, 1977).

Table 5. Observed cation ratios in clinoptilolite (Cp) of the Sucker Creek Formation and calculated cation ratios and total dissolved solids (TDS) of associated fluids.[1]

	12-86-D (K-Cp)	26-86-E (K-Cp)	7-87-F (Ca-Cp)
K/Na/Ca/Mg (mineral)	1/.71/.48/.17	1/.23/.11/0	1/4.0/6.1/1.7
K/Na/Ca/Mg (fluid)	1/57.1/23.8/9.2	1/18.5/5.4/0	1/318/305/9.2
log(Na + K)/(Ca + Mg) (fluid)	0.25	0.56	0.01
TDS (ppm)	400	560	320

[1] See text for calculation procedure.

A simple downward pathway for hydrologic flow could produce vertical gradients in solution composition and mineralogy with the idealized zonation consisting of fresh glass at the top of the section, clinoptilolite (± smectite) at intermediate depths, and perhaps analcime (±K-feldspar) at the deepest intervals. Ancient examples of hydrologically open systems include Yucca Mountain, Nevada (Miocene, Broxton *et al.*, 1987) and the John Day Formation, Oregon (Miocene–Oligocene, Hay, 1963).

Although the physiography of the depositional environment of the Sucker Creek Formation (basin and range) is appropriate for the possible development of a closed hydrologic system, the above data suggest an open hydrologic system for the development of the clinoptilolite facies. First, the Sucker Creek Formation was deposited in a moist, temperate lowland climate (Kittleman, 1973), not an arid to semi-arid climate, which is important for the development of a playa environment. Second, no saline minerals, such as trona or gaylussite, were observed; in fact, calcite is present as a silty limestone below the clinoptilolite in section D. Third, no major lateral zonation in mineralogy was observed over the 30-km outcrop width, but vertical zonations were observed on an outcrop scale with a smectite-rich horizon (+clinoptilolite) at the top of the outcrop and a clinoptilolite-rich horizon (+smectite) at the bottom of the outcrop. Between these horizons substantially unaltered ash (0.5–2-mm grain size) is present, which may represent a coarse-grained layer in which water was able to pass through rapidly without producing much alteration. Fourth, zeolites, such as analcime, chabazite, erionite, and phillipsite, which commonly form in closed hydrologic systems (Surdam, 1977), were not observed in this study. Fifth, calculated fluid compositions based on a procedure described in Boles and Surdam (1979) are relatively dilute (400–600 ppm, Table 5). The calculation procedure involves determination of the molar ratio of K/Na/Ca/Mg in the fluid based on the observed molar ratio of K/Na/Ca/Mg in the clinoptilolite (data in Table 3) and assumed fractionation factors between clinoptilolite and fluid. Boles and Wise (1978) determined that Na, Ca, and Mg are enriched in the fluid phase relative to K by factors of 80, 50, and 55, respectively. The calculated molar ratio of (Na + K)/(Ca + Mg) in the fluid gives an estimate of total dissolved solids in the fluid using data from Jones (1965) (Figure 7 in Boles and Surdam, 1979).

We propose that the Ca-clinoptilolite-rich tuffs (section F) initially altered to K-clinoptilolite in an open hydrologic system and then were subjected to a later low-temperature hydrothermal event (perhaps 75°–150°C), probably related to later volcanic activity, such as extrusion of the Owyhee basalt or the Jump Creek rhyolite (Kittleman *et al.*, 1965). The evidence for the initial alteration stage is the textural similarity between the K- and Ca-clinoptilolite-rich tuffs, e.g., zeolites in both tuffs replace shards and fill cavities. The later hydrothermal event is perhaps best evidenced by the presence of authigenic quartz and absence of opal-CT in Ca-clinoptilolite tuffs. The acicular morphology of the quartz is similar to acicular opal-CT, common in the K-clinoptilolite-rich tuffs, and suggests recrystallization of quartz from an opal-CT precursor. Temperatures for the opal-CT reaction to quartz for Miocene-age strata are about 75°–110°C (Murata and Larson, 1975). The Ca-rich composition of the clinoptilolite is compatible with hydrothermal activity, because Ca-rich clinoptilolite is an uncommon alteration product in low-temperature open hydrologic systems (Hay, 1977). Because Si/Al ratios for K- and Ca-clinoptilolite are similar (Table 3), the postulated hydrothermal event only affected the exchangeable cations in the zeolite. Based on the cation composition of Ca-clinoptilolite, the hydrothermal fluids appear to have been dilute (~300 ppm, Table 5). Finally, the presence of illite is also compatible with hydrothermal activity, but, because we could not positively identify illite by SEM, we do not know whether it is detrital or authigenic.

CONCLUSIONS

The observed mineralogical, chemical, and textural variations in tuffs of the Sucker Creek Formation in eastern Oregon are the result of differences in the composition of the volcanic precursor and the diagenetic fluids. Bentonite was probably derived from dacitic volcanic ash, which was deposited in lakes and subsequently altered during diagenesis by dilute fluids in a relatively closed chemical system. Silica in adjacent opal-CT beds was derived chiefly from the conversion

of ash to smectite. K- and Ca-clinoptilolite-rich tuffs were derived from rhyolitic ash and subjected to diagenetic alteration in an open hydrologic system. K-clinoptilolite apparently underwent additional alteration by low-temperature hydrothermal fluids (perhaps 75°–150°C), which caused Ca-for-(K + Na) exchange and reaction of opal-CT to quartz.

ACKNOWLEDGMENTS

We thank Glen Teague and David Leppert of Teague Minerals Products Company (Adrian, Oregon) for their invaluable assistance in the field studies, for helpful manuscript reviews, and for stimulating discussions. We also thank R. L. Hay and R. H. Lander for extremely helpful discussions, D. L. Bish for the Rietveld refinements, J. R. Boles, D. B. Hawkins, F. A. Mumpton, and R. A. Sheppard for thorough manuscript reviews, R. H. Lander for microprobe analyses, E. J. Daniels for assistance in sample preparation, and J. Knox for preparation of figures. This work was funded by the National Science Foundation through grant EAR-87-07319 and by the Petroleum Research Fund through grant 18685-G2.

REFERENCES

Appleman, D. E. and Evans, H. T., Jr. (1973) Indexing and least-squares refinement of powder diffraction data: *U.S. Dept. of Commerce Natl. Tech. Serv. Publ.* **PB 216-188,** 62 pp.

Bayliss, P. (1986) Quantitative analysis of sedimentary minerals by powder X-ray diffraction: *Powd. Diff.* **1,** 37–39.

Boles, J. R. and Surdam, R. C. (1979) Diagenesis of volcanogenic sediments in a Tertiary saline lake; Wagon Bed Formation, Wyoming: *Amer. J. Sci.* **111,** 832–853.

Boles, J. R. and Wise, W. S. (1978) Nature and origin of deep-sea clinoptilolite: in *Natural Zeolites: Occurrence, Properties, Use,* L. B. Sand and F. A. Mumpton, eds., Pergamon Press, Elmsford, New York, 235–243.

Broxton, D. E., Bish, D. L., and Warren, R. G. (1987) Distribution and chemistry of minerals at Yucca Mountain, Nye County, Nevada: *Clays & Clay Minerals* **35,** 89–110.

Drever, J. I. (1988) *The Geochemistry of Natural Waters:* Prentice Hall, Englewood Cliffs, New Jersey, 437 pp.

Fisher, R. V. and Schmincke, H.-U. (1984) *Pyroclastic Rocks:* Springer Verlag, New York, 472 pp.

Gottardi, G. and Galli, G. (1985) *Natural Zeolites:* Springer Verlag, New York, 409 pp.

Hay, R. L. (1963) Stratigraphy and zeolitic diagenesis of the John Day Formation of Oregon: *Calif. Univ. Pub. Geol. Soc.* **42,** 199–262.

Hay, R. L. (1966) Zeolites and zeolitic reactions in sedimentary rocks: *Geol. Soc. Amer. Spec. Pap.* **85,** 130 pp.

Hay, R. L. (1977) Geology of zeolites in sedimentary rocks: in *Mineralogy and Geology of Natural Zeolites,* F. A. Mumpton, ed., *Reviews in Mineralogy* **4,** Mineral. Soc. Amer., Washington, D.C., 53–64.

Hay, R. L. and Guldman, S. G. (1987) Diagenetic alteration of silicic ash in Searles Lake, California: *Clays & Clay Minerals* **35,** 449–457.

Hay, R. L., Pexton, R. E., Teague, T. T., and Kyser, T. K. (1986) Spring-related carbonate rocks, Mg clays, and associated minerals in Pliocene deposits of the Armagosa Desert, Nevada and California: *Geol. Soc. Amer. Bull.* **97,** 1488–1503.

Hay, R. L. and Sheppard, R. A. (1977) Zeolite in open hydrologic systems: in *Mineralogy and Geology of Natural Zeolites,* F. A. Mumpton, ed., *Reviews in Mineralogy* **4,** Mineral. Soc. Amer., Washington, D.C., 93–102.

Hoffman, J. (1976) Regional metamorphism and K-Ar dating of clay minerals in Cretaceous sediments of the disturbed belt of Montana: Ph.D. dissertation, Case-Western Reserve University, Cleveland, Ohio, 266 pp.

Jones, B. F. (1965) The hydrology and mineralogy of Deep Springs Lake, Inyo County, California: *U.S. Geol. Surv. Prof. Pap.* **502-A,** 56 pp.

Kittleman, L. R. (1973) Guide to the geology of the Owyhee region of Oregon: *Univ. Oregon Mus. Nat. Hist. Bull.* **21,** 61 pp.

Kittleman, L. R., Green, A. R., Hagood, A. R., Johnson, A. M., McMurray, J. M., Russell, R. G., and Weeden, D. A. (1965) Cenozoic stratigraphy of the Owyhee region, southeastern Oregon: *Univ. Oregon Mus. Nat. Hist. Bull.* **1,** 45 pp.

Leppert, D. (1990) Developments in applications for southeast Oregon bentonites and natural zeolites: in *Proc. 25th Forum of Geol. of Ind. Min.,* R. P. Geitgey and B. F. Vogt, eds., Oreg. Dept. of Geol. and Min. Ind. Spec. Pap. **23,** 19–23.

Murata, K. J. and Larson, R. R. (1975) Diagenesis of Miocene siliceous shales, Tremblor Range, California: *U.S. Geol. Surv. J. Res.* **3,** 553–566.

Reynolds, R. C. (1989) Principles and techniques of quantitative analysis of clay minerals by X-ray powder diffraction: in CMS Workshop Lectures, Vol. 1, *Quantitative Mineral Analysis of Clays,* D. R. Pevear and F. A. Mumpton, eds., The Clay Minerals Society, Evergreen, Colorado, 4–36.

Ross, C. S. and Hendricks, S. B. (1945) Minerals of the montmorillonite group: *U.S. Geol. Surv. Prof. Pap.* **205B,** 77 pp.

Shepard, A. O. and Starkey, H. C. (1966) The effects of exchanged cations on the thermal behaviour of heulandite and clinoptilolite: *Int. Mineral. Assoc. Vol.,* Mineral. Soc. India, 155–158.

Sheppard, R. A. and Gude, A. J., 3rd (1968) Distribution and genesis of authigenic silicate minerals in tuffs of Pleistocene Lake Tecopa, Inyo County, California: *U.S. Geol. Surv. Prop. Pap.* **597,** 38 pp.

Sheppard, R. A. and Gude, A. J., 3rd (1973) Zeolites and associated authigenic silicate minerals in tuffaceous rocks of the Big Sandy Formation, Mohave County, Arizona: *U.S. Geol. Surv. Prof. Pap.* **830,** 36 pp.

Slaughter, M. and Earley, J. W. (1965) Mineralogy and geological significance of the Mowry bentonites, Wyoming: *Geol. Soc. Amer. Spec. Pap.* **83,** 116 pp.

Surdam, R. C. (1977) Zeolites in closed hydrologic systems: in *Mineralogy and Geology of Natural Zeolites,* F. A. Mumpton, ed., *Reviews in Mineralogy* **4,** Mineral. Soc. Amer., Washington, D.C., 65–91.

Surdam, R. C. and Parker, R. B. (1972) Authigenic aluminosilicate minerals in the tuffaceous rocks of the Green River Formation, Wyoming: *Geol. Soc. Amer. Bull.* **83,** 689–700.

Taylor, M. W. and Surdam, R. C. (1981) Zeolite reactions in the tuffaceous sediments at Teels Marsh, Nevada: *Clays & Clay Minerals* **29,** 341–352.

Wiles, D. B. and Young, R. A. (1981) A new computer program for Rietveld analysis of X-ray powder diffraction patterns: *J. Appl. Crystallogr.* **14,** 149–151.

(Received 19 July 1989; accepted 5 August 1990; Ms. 1925)